

Vacancy formation energy near an edge dislocation: A hybrid quantum-classical study

F. Tavazza, R. Wagner, A.M. Chaka, L.E. Levine*

National Institute of Standards and Technology, Gaithersburg, MD 20899, USA

Received 13 September 2004; received in revised form 1 February 2005; accepted 28 March 2005

Abstract

In this work, the formation energy of a single vacancy in aluminum at different distances from an edge dislocation core is studied using a new, hybrid *ab initio*-classical potential methodology. Such an approach allows us to conduct large-scale atomistic simulations with a simple classical potential (embedded atom method (EAM), for instance) while simultaneously using the more accurate *ab initio* approach (first principles quantum mechanics) for critical embedded regions. The coupling is made through shared shells of atoms where the two atomistic modeling approaches are relaxed in an iterative, self-consistent manner. The small, critical region is relaxed using all electron density functional theory (DFT) and the much larger cell in which this is embedded is relaxed using a minimization algorithm with EAM potentials.

© 2005 Elsevier B.V. All rights reserved.

Keywords: Vacancy formation; Al; Electron density functional theory; Embedded atom method

1. Introduction

Understanding dislocation behavior is a key for designing materials with improved properties; however, despite a massive body of literature [1], much is still unknown about the subject. In this work, the formation energy of a vacancy in the proximity of an edge dislocation is analyzed, together with the atomic relaxations that occur near the vacancy itself. To determine the behavior of the formation energy as a function of the distance from the dislocation, it is necessary to simulate reasonably large systems, so that several distances could be studied. The *ab initio* methods usually utilized to investigate dislocation cores [2–9] currently do not allow treatment of systems large enough for our purposes. Empirical techniques are fast enough to treat millions of atoms, but are intrinsically limited by the approximations made in constructing the potentials, and hence, may be inadequate for the accurate determination of the properties under examination.

To overcome such an impasse, we utilize a hybrid quantum-classical algorithm that is designed to conduct

large-scale atomistic simulations with simple classical potentials while simultaneously using the more accurate *ab initio* approach for critical embedded regions. This methodology allows us to take advantage of the accuracy of the density functional theory (DFT) calculations in the region of interest, while the large, classical, embedding cell eliminates concerns related to the effect of cluster termination on a small system and the necessity of artificially including long range elastic effects as required by the presence of a dislocation. In most hybrid methods, the shaking-hand zone is given by an interface ([10,11] for instance); on one side of the interface the bonds are derived from the *ab initio* (or tight-binding) Hamiltonian, while on the other side they are derived from a classical interatomic potential. In our method, the shaking-hand zone is a shell several Angstrom thick whose atoms are moved, iteratively, both classically and quantum-mechanically. The most significant difference between this algorithm and other hybrid methods, though, is the fact that we consider a critical region large enough to include most of the effect of any desired perturbation. This requirement guarantees that outside the critical region the description of the material provided by the classical approximation is very similar to that due to the quantum approach. It also means that we are not extremely

* Corresponding author. Fax: +1 301 975 4553.

E-mail address: lyle.levine@nist.gov (L.E. Levine).

sensitive to the quality of the classical potential employed because it is only used away from the zone of interest.

2. Simulation methodology

The idea behind this hybrid quantum-classical approach is to consider a critical region large enough to include most of the effect of whatever perturbation we wish to introduce in the system (the vacancy, for example).

The coupling between the ab initio and the classical simulations is made through shared atomic shells where the two atomistic approaches are used in an iterative, self-consistent manner. The small, critical region is relaxed using density functional theory and the much larger cell in which this is embedded is relaxed using a minimization algorithm. Both relaxations are repeated until convergence is achieved. The DFT sphere is composed of three concentric shells, labeled “1”, “2” and “3” in Fig. 1(b): all the atoms contained in shells 1 and 2 are allowed to relax during the DFT calculation, while those in shell 3 are kept fixed in positions determined by the previous classical run. During each classical relaxation, atoms in shell 1 are kept fixed in positions determined by the previous DFT relaxation, while atoms in shells 2, 3, and 4 are allowed to relax. Atoms in shell 5 are kept fixed at all times in their initial positions because they constitute the most external shell of the classical cluster. More details on the method are given in references [12,13], including convergence tests in critical region size and hand-shake region thickness. All the results discussed in this paper were obtained considering large enough regions, for both areas, to ensure such a convergence.

The classical simulations are conducted using the Ercolessi–Adam embedded atom potential (EAM) [14] for aluminum, with parameters as determined by Liu et al. [15]. The classical simulation cell consists of $16 \times 16 \times 12$ repetitions of a conventional cell containing 12 atoms and constructed along the $[\bar{1} 1 0]$, $[1 1 1]$ and $[1 1 \bar{2}]$ directions (direction x , y and z in the rest of the paper, respectively) [16]. For the classical cell, periodic boundary conditions (PBC) were introduced in the direction of the dislocation line (z) only, while along x and y a cluster termination was used (Fig. 1(a)). The edge dislocation has a line sense direction $[1 1 \bar{2}]$, slip plane $(1 1 1)$ and Burgers vector $[\bar{1} 1 0]$. The DFT calculations are performed on a cluster configuration (a sphere), so that no k -point sampling is required. We utilized DMol³ [17] and an all-electron, generalized gradient approximation (GGA) approach (Perdew–Burke–Ernzerhof [18]), with a real-space cutoff of 0.4 nm and a numerical, double-zeta, atom centered basis (dnd). The DFT cluster contained 248 atoms, of which 43 were relaxed during the DFT simulations. The initial atomic positions come from the elastic displacement fields provided by standard elasticity theory for an infinitely long, straight edge dislocation [19]. Before starting the hybrid calculations, the relaxed volume for the simulation cell was determined using a constant pressure, off-lattice,

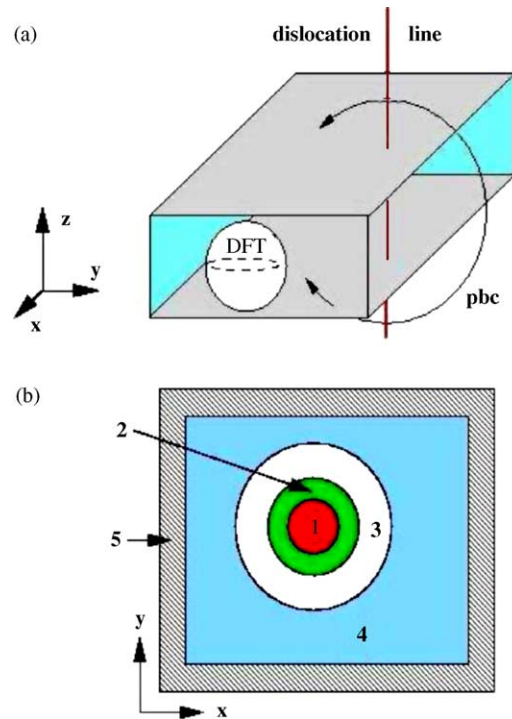


Fig. 1. (a) Example of simulation cell: the gray parallelepiped constitutes the classical cell inside which is the critical region (spherical region marked “DFT”). (b) Schematic 2D representation of the shell structure. Shells 1, 2, and 3 correspond to the critical region, i.e. are considered in the DFT calculation. During the classical relaxation all shells are considered, but only atoms in shells 2, 3 and 4 are allowed to move.

standard Metropolis Monte Carlo at very low temperature ($T = 5$ K).

3. Results

To study the formation energy of a vacancy near an edge dislocation, we analyzed six different vacancy locations, all of them roughly positioned on the same straight line (direction $[\bar{3} 1 \bar{7} 1 0]$), in the tensile part of the crystal and with a distance from the core ranging from 1.6 nm (V_1) to 5.2 nm (V_7) (Fig. 2).

As shown in Fig. 3a, our results can be well fitted using a hyperbolic function (reduced $\chi^2 = 1.9 \times 10^{-6}$ at small distances). The fitting allows estimation of the formation energy at closer distances to the core obtaining, for instance, an extrapolated value of 1.05 eV at 0.25 nm. Remembering that the formation energy of a vacancy in Al bulk is 0.69 eV [15], this corresponds to an increase of about 50%, in very good agreement with what was suggested by Balluffi and Granato [20]. In Fig. 3b, the hybrid results are compared to purely classic calculations (performed using the same minimization code we used in the classical part of the hybrid algorithm). The only-classical results are shifted so that the formation energy at infinite distance from the dislocation coincides with the one found using the hybrid method. It appears that suffi-

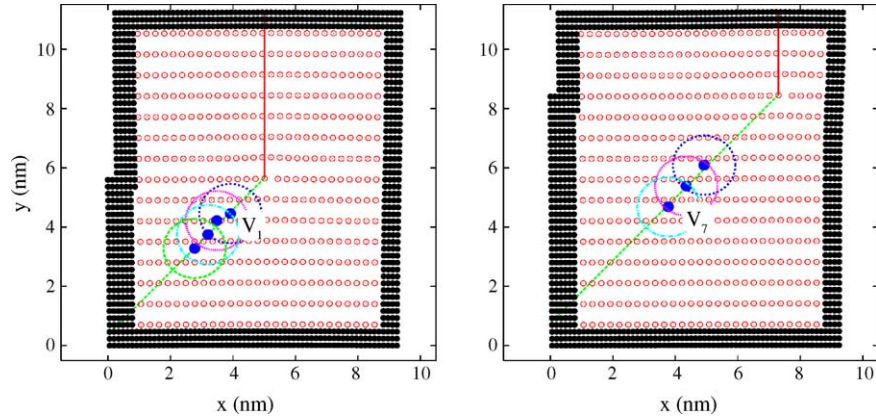


Fig. 2. Vacancy positions for our simulations. Seven different locations for the vacancy are shown, where V_1 is the closest to the dislocation, V_7 the furthest. The dashed circles represent the xy -projection of the critical region around each vacancy location. For clarity, only one atomic plane is shown inside the cell, while atoms on all planes are displayed in the area corresponding to shell 5, i.e. where the atoms are kept fixed at all times.

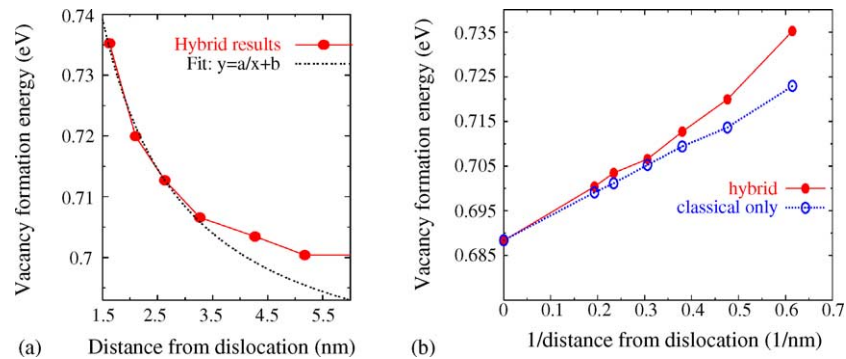


Fig. 3. Hybrid vacancy formation energies as a function of the distance (a) and of the inverse of the distance (b) from the dislocation core. In (a), the fitting function $f(x) = a/x + b$ is also shown. In (b), the corresponding classical-only results are also shown (the classical energies are translated so that the value for $x = 0$ (i.e. no vacancy) coincides with that obtained in the hybrid case).

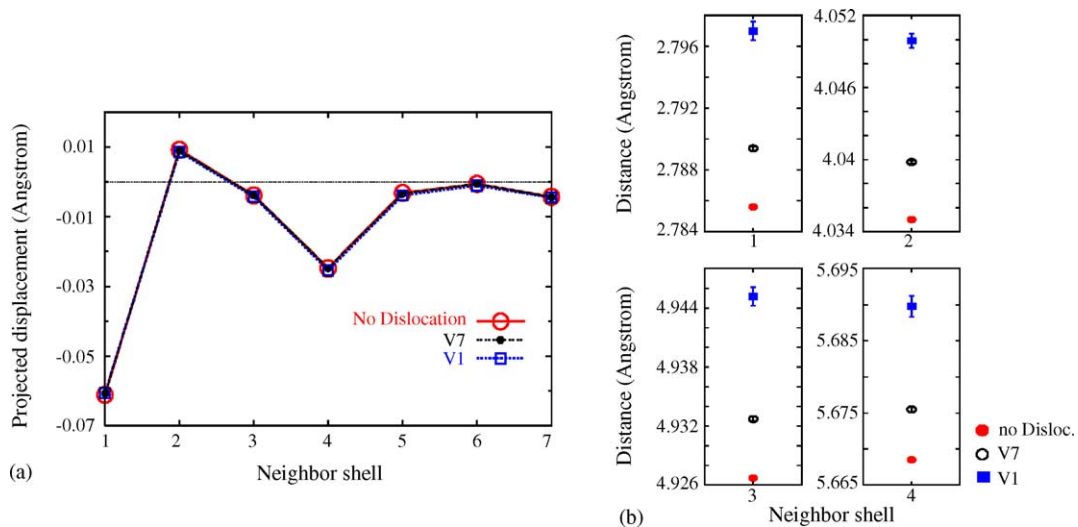


Fig. 4. Projected atomic relaxation around the vacancy (a) and vacancy-neighbor shell distances (b) for vacancy V_1 (distance from the core = 1.6 nm), V_7 (distance from the core = 5.2 nm) and in the absence of the dislocation. In (b), each data point is given by the average of all the distances in that neighbor shell; where not shown, the error-bars are smaller than the symbol.

ciently far from the dislocation the two approaches coincide, in agreement with what is ordinarily found. At shorter distances, though, the two results diverge, possibly explaining why previous classical-only calculations [21,22] failed to find a monotonically increasing energy as the distance from the core diminishes. More details on the energy calculation are given in [12].

Lastly, we examined the atomic relaxations around the vacancy. The atomic displacements along the relaxation directions that are followed in the case of a single vacancy in an otherwise perfect crystal (i.e. without dislocations) are shown in Fig. 4a. There are no significant differences between the three cases, indicating that at the analyzed distances the effect of the vacancy is much stronger than that of the dislocation. This, though, does not mean that the environment around the vacancy is identical in all three cases, i.e. that the dislocation has no effect at all; as shown in Fig. 4b, the average distance between the vacancy and its first four shells of neighbors is different in the three cases. The error-bar on the average distance (due to the distribution of the distances in each neighboring shell) is also always larger in the case of the vacancy being closer to the core (V_1), which is consistent with a larger effect of the dislocation. Our results for the projected atomic displacements are in very good agreement with what is commonly found for an Al vacancy in a perfect crystal [23].

4. Conclusions

In this paper, we apply a new, hybrid quantum-classical methodology to the study of vacancy formation energies at different distances from a dislocation core. Results consistent with expected behaviors are found, that validate the methodology both qualitatively and quantitatively.

References

- [1] F.R. Nabarro (Ed.), *Dislocations in Solids*, North-Holland, New York, 1979–1996 (and references therein).
- [2] S. Rao, C. Hernandez, et al., *Phil. Mag. A* 77 (1998) 231.
- [3] C. Woodward, S.I. Rao, *Phil. Mag. A* 81 (2001) 1305.
- [4] C. Woodward, S.I. Rao, *Phys. Rev. Lett.* 88 (2002) 216402–216411.
- [5] J.R.K. Bigger, D.A. McInnes, A.P. Sutton, et al., *Phys. Rev. Lett.* 69 (1992) 2224.
- [6] N. Letho, S. Oberg, *Phys. Rev. Lett.* 80 (1998) 5568.
- [7] S. Ismail-Beigi, T.A. Arias, *Phys. Rev. Lett.* 84 (2000) 1499.
- [8] T.A. Arias, J.D. Joannopoulos, *Phys. Rev. Lett.* 73 (1994) 680.
- [9] J. Bennetto, et al., *Phys. Rev. Lett.* 79 (1997) 245.
- [10] S. Ogata, F. Shimojo, R.K. Kalia, A. Nakano, P. Vashishta, *J. Appl. Phys.* 95 (2004) 39409.
- [11] N. Bernstein, D. Hess, *Mat. Res. Soc. Symp. Proc.* 653 (2001) Zz2.7.1.
- [12] F. Tavazza, A.M. Chaka, L.E. Levine, *Computational Modeling and Simulation of Materials III Part A*, Cimtec-Techna Group, 2004, p. 657.
- [13] F. Tavazza, A.M. Chaka, L.E. Levine, private communication.
- [14] F. Ercolessi, J.B. Adam, *Europhys. Lett.* 26 (1994) 583.
- [15] X.-Y. Liu, et al., *Surf. Sci.* 373 (1997) 357.
- [16] Q.F. Fang, R. Wang, *Phys. Rev. B* 62 (2000) 9317.
- [17] B. Delley, *J. Chem. Phys.* 92 (1990) 508.;
B. Delley, *J. Chem. Phys.* 113 (2000) 7756.
- [18] J.P. Perdue, K. Burke, M. Ernzerhof, *Phys. Rev. Lett.* 77 (1996) 3865.
- [19] J.P. Hirth, J. Lothe, *Theory of Dislocations*, second ed., Krieger, Malabar, 1992.
- [20] R.W. Baluffi, A.V. Granato, in: F.R.N. Nabarro (Ed.), *Dislocation in Solids*, vol. 4, North-Holland, Amsterdam, 1979, p. 1.
- [21] M. Doyama, R.M.J. Cotterill, *Suppl. Trans. Jpn. Inst. Met.* 9 (1968) 55.
- [22] R. Bullough, R.C. Perrin, in: A.R. Rosenfield, et al. (Eds.), *Dislocation Dynamics*, McGraw-Hill, New York, 1968, p. 175.
- [23] D.E. Turner, Z.Z. Zhu, C.T. Chan, K.M. Ho, *Phys. Rev. B* 55 (1997) 13842.